NMR Chemical-Shift Anomaly and Bonding in Piano-Stool Carbonyl and Related Complexes—An Ab Initio ECP/DFT Study

Martin Kaupp*

Dedicated to Professor Hans Georg von Schnering on the occasion of his 65th birthday

Abstract: The origin of the unusually large carbonyl ^{13}C shifts and of unusual periodic trends in four-legged piano-stool complexes $[M(\eta^5\text{-}C_5H_5)(CO)_4]^-$ (M = Ti, Zr, Hf) and in related species has been investigated by using a combination of ab initio effective-core potentials (ECPs) and density-functional theory (DFT). The ECP/SOS-DFPT(IGLO) calculations indicate a considerable reduction in the anisotropy of the $^{13}C(CO)$ chemical shift tensors compared to terminal carbonyl ligands in "normal" complexes. This is due to large paramagnetic contributions from metal d AO type (d_{z^2}, d_{xy}) orbitals to the parallel component, σ_{33}, of the shielding tensors of the carbonyl carbon atoms. The neutral d^4 Group 5 and 6 complexes $[M(\eta^5\text{-}C_5H_5)(CO)_4]$ (M = V, Nb, Ta) and $[M(\eta^5\text{-}C_5H_5)(CO)_3CH_3]$ (M = Cr, Mo, W) exhibit successively smaller but still significant paramagnetic d-orbital contributions to σ_{33}, consistent with the observed less dramatic deshielding. The three-legged d^6 piano-stool complexes $[M(\eta^5\text{-}C_5H_5)(CO)_3]$ (M = Mn, Tc, Re) do not exhibit these reductions of the shielding anisotropy, but have carbonyl ^{13}C shift tensors comparable to regular octahedral carbonyl complexes. The special situation for the four-legged complexes is related to the presence of high-lying occupied metal d orbitals, and particularly to the favorable spatial arrangement of these d orbitals with respect to the carbonyl ligands. Bent-sandwich d^2 complexes like $[Zr(\eta^5\text{-}C_5H_5)_2(CO)_2]$ exhibit comparable deshielding contributions from an occupied metal d orbital. For similar reasons, the ^{17}O resonances for these piano-stool and bent-sandwich complexes are also predicted to be at unusually high frequencies, with low shift anisotropy. NMR shifts for the $(\eta^5\text{-}C_5H_5)$-ligand atoms and the structures of the complexes are also discussed.

Keywords
carbonyl complexes · density-functional theory · NMR chemical shifts · pseudopotentials · transition-metal complexes

Introduction

Complementary to the $\tilde{\nu}(CO)$ vibrational frequencies, the ^{13}C NMR chemical shifts are the most important experimental probes for the molecular and electronic structures in transition-metal carbonyl complexes. The ^{13}C chemical shifts of terminal carbonyl groups in transition-metal complexes typically range from approximately $\delta = 170$ to 240 (vs. TMS).[1-4] However, during the last decade, several groups have prepared and characterized carbonyl complexes of the early transition metals with terminal carbonyl ^{13}C resonances in the range of $\delta = 260$ to 320 (cf. Table 1),[5-11] that is, with chemical shifts that are more characteristic for bridging rather than for terminal CO ligands.

Most of these compounds are four-legged piano-stool d^4[5-7] or bent-sandwich d^2 complexes[8, 9] of the Group 4 metals Ti, Zr, and Hf (Table 1). These complexes have very electron-rich metal centers and a high degree of $M \rightarrow C{\equiv}O$ backbonding, as indicated by their relatively low carbonyl IR frequencies.[5-10] Therefore, the large $\delta\,^{13}C(CO)$ has been related to backbonding.[5e, f, 7] However, there are several indications[5e,f] that this

Table 1. Examples of unusually large $\delta(^{13}CO$ terminal) in transition-metal carbonyl complexes [a].

	$\delta(^{13}CO)$	Ref.		$\delta(^{13}CO)$	Ref.
$[TiCp(CO)_4]^-$	289	[5a,b,e,f]	$[Zr(\eta^5\text{-}C_5R_5)(CO)_2(dmpe)Cl]$	279	[5e]
$[ZrCp(CO)_4]^-$	292	[5a,b,e]	$[Hf(\eta^5\text{-}C_5R_5)(CO)_2(dmpe)Cl]$	283	[5e]
$[HfCp(CO)_4]^-$	291	[5d,e]	$[\{HB(Pz)_3\}Ti(CO)_4]^-$	286	[5g]
$[Ti(\eta^5\text{-}C_5Me_5)(CO)_4]^-$	293	[5a,b,e,f]	$[Ti(trmpe)(CO)_4]$	278	[6]
$[Zr(\eta^5\text{-}C_5Me_5)(CO)_4]^-$	296	[5a,b,e]	$[Zr(trmpe)(CO)_4]$	284	[6]
$[Hf(\eta^5\text{-}C_5Me_5)(CO)_4]^-$	296	[5d,e]	$[Hf(trmpe)(CO)_4]$	282	[6]
$[Ti(Ind)(CO)_4]^-$	289	[5g]	$[Ti(trimpsi)(CO)_4]$	277	[7]
$[Ti(\eta^5\text{-}C_5R_5)(CO)_3PR_3]^-$	299-308	[5f]	$[ZrCp_2(CO)_2]$	265	[8]
$[Ti(\eta^5\text{-}C_5R_5)(CO)_2(dmpe)]^-$	311-320	[5f]	$[MCp_2(CO)L]$ [b]	260-311	[9,10]
$[Ti(\eta^5\text{-}C_5R_5)(CO)_3PR_3H]$	267-273	[5f]	$[V(CO)_5]^{3-}$	290	[11]
$[Ti(\eta^5\text{-}C_5R_5)(CO)_2(dmpe)H]$	267	[5c]	$[Ta(CO)_5]^{3-}$	293	[11]
$[Ti(\eta^5\text{-}C_5R_5)(CO)_2(dmpe)I]$	267,254	[5e]			

[a] In ppm vs. TMS. R = H, CH_3; dmpe = 1,2-bis(dimethylphosphino)ethane; Ind = indenyl; Pz = pyrazolyl; trimpsi = tBuSi($CH_2PMe_2)_3$; trmpe = 1,1,1-tris(dimethylphosphinomethyl)ethane; Cp = η^5-C_5H_5. [b] M = Ti, Zr, Hf; L = PMe_3, $P(OMe)_3$, CNR, η^2-$Me_2SiNtBu$.

[*] Dr. Martin Kaupp
Max-Planck-Institut für Festkörperforschung
Heisenbergstrasse 1, D-70569 Stuttgart (Germany)
Fax.: Int. code + (711)689-1562
email: kaupp@vsibm1.mpi-stuttgart.mpg.de
and
Institut für Theoretische Chemie, Universitaet Stuttgart
Pfaffenwaldring 55, D-70569 Stuttgart (Germany)
Fax.: Int. code + (711)685-4442

0947-6539/96/0203-0348 $ 15.00+.25/0 Chem. Eur. J. 1996, 2, No. 3

does not sufficiently explain the exceptionally large carbonyl ^{13}C NMR shifts:

1) The trends in $^{13}C(CO)$ chemical shifts are not always related to those of the IR frequencies. Thus, for example, the carbonyl ^{13}C shifts in the half-sandwich carbonyl anions $[FeCp(CO)_2]^-$, $[CrCp(CO)_3]^-$, and $[TiCp(CO)_4]^-$ ($Cp = \eta^5$-C_5H_5) span a very large range, while the IR-active $\tilde{\nu}(CO)$ values for these three species are similar (cf. Table 2).[5f]
2) There are a number of complexes closely related to those with the unusually high ^{13}C shifts, such as $[Hf(1,3,5\text{-}tBu_3C_6H_3)_2(CO)]$[12] or the highly reduced carbonyl anions $[M(CO)_6]^{2-}$ (M = Ti, Zr, Hf),[13] which exhibit much lower $\delta\,^{13}C(CO)$ values ($\delta \approx 240-250$). Note that the latter dianions have very low values for $\tilde{\nu}(CO)$ (ca. 1750 cm^{-1}), consistent with appreciable backbonding (Table 2).

Table 2. Lack of correlation between ^{13}C shifts and IR frequencies.

compound	$\delta(^{13}CO)$ (ppm)	$\tilde{\nu}(CO)$ (cm^{-1})
$[FeCp(CO)_2]^-$	230 [a]	1865(s), 1788(s) [b]
$[CrCp(CO)_3]^-$	247 [c]	1880, 1770 [d]
$[TiCp(CO)_4]^-$	289 [e]	1921(m), 1777(s) [e]
$[Ti(CO)_6]^{2-}$	246 [f]	1748(vs) [f]
$[Zr(CO)_6]^{2-}$	245 [f]	1757(vs) [f]
$[Hf(CO)_6]^{2-}$	244 [f]	1757(vs) [f]

[a] Y. Wielstra, S. Gambarotta, J. B. Roedelof, M. Y. Chiang, *Organometallics* **1988**, *7*, 2177. [b] J. E. Ellis, E. A. Flom, *J. Organomet. Chem.* **1975**, *99*, 263. [c] G. M. Bodner, L. J. Todd, *Inorg. Chem.* **1974**, *13*, 1335. [d] P. Hackett, P. S. O'Neill, A. R. Manning, *J. Chem. Soc. Dalton Trans.* **1974**, 1625. [e] Ref. [5e]. [f] Ref. [13].

3) Normally, ^{13}C shifts for terminal CO ligands decrease upon descending a given triad, for example, $\delta = 212$, 204, and 192 for $Cr(CO)_6$, $Mo(CO)_6$, and $W(CO)_6$, respectively.[1] However, in cases where all Group 4 piano-stool complexes for a given set of ligands have been studied, namely, for $[MCp(CO)_4]^-$,[5] $[M\{C_5(CH_3)_5\}(CO)_4]^-$,[5] and $[M(trmpe)(CO)_4]$ (M = Ti, Zr, Hf),[6] $\delta\,^{13}C(CO)$ for the titanium complex is very similar to and even slightly smaller than that for the corresponding Zr and Hf analogues (cf. Table 1).

These pecularities suggest that there is something special about the mechanisms determining $\delta\,^{13}C(CO)$ in the Group 4 piano-stool d^4 and bent-sandwich d^2 carbonyl complexes. To increase our understanding of the unusual NMR features and the bonding in these compounds, as well as of the rules governing NMR shifts in transition-metal carbonyl complexes in general, we have carried out ab initio calculations of the NMR chemical shift tensors for the ligands in $[MCp(CO)_4]^-$ (M = Ti, Zr, Hf), and in many related species.

We have used quasirelativistic ab initio effective-core potentials (ECPs)[14] for the metals together with sum-over-states density functional perturbation theory (SOS-DFPT).[15] This combination of methods has recently been shown to be the first approach that yields accurate isotropic shieldings and shielding tensors for ligand atoms in transition-metal complexes.[16–18] The calculated shielding tensors may then be analyzed in terms of contributions from localized molecular orbitals (LMOs), or be broken down into contributions from individual electronic excitations to the sum-over-states expression. We find that paramagnetic contributions from nonbonding metal d orbitals are responsible for the unusual deshielding in the four-legged complexes. This leads to a number of generalizations that should help in the prediction of shifts.

Half-sandwich carbonyl complexes of the piano-stool type are important organometallic reagents. The bonding in this class of compounds has been studied extensively, usually at semiempirical levels of theory.[19–21] This previous work will be referred to in detail in our bonding interpretations (Section 5).

Computational Methods

For consistency (experimental structures were not available for all species), all structures of the piano-stool complexes were fully optimized at the gradient-corrected density-functional theory (DFT) level, using the Becke-Perdew exchange-correlation functional combination [22] (experimental structures were only used for $[ZrCp_2(CO)_2]$ and for $[M(CO)_6]^{2-}$ (M = Ti, Zr, Hf); cf. Sections 7 and 8, respectively). The optimizations were carried out without any symmetry restrictions. Quasirelativistic energy-adjusted metal ECPs and (8s7p6d)/[6s5p3d] GTO valence basis sets [14] were used. For comparison, in the cases of $[HfCp(CO)_4]^-$ and $[ReCp(CO)_3]$, nonrelativistic metal-ECP [14b] calculations were also carried out. In the optimizations, ECPs were also used for C and O, with (4s4p1d)/[2s2p1d] valence bases [23]. A (4s)/[2s] basis[24] was employed for hydrogen. The ECPs have been transformed to nonlocal form [25] for technical reasons [26]. The transferability of this type of ab initio ECPs into DFT applications has been studied in detail and was found to be excellent [16–18,26,27]. Auxiliary basis sets [28] for the fit of the exchange-correlation potential and of the charge density were of the sizes 3,4 for the metals, 3,3 for carbon and oxygen, and 4,0 for hydrogen (*n,m* stands for *n* s functions and *m* spd shells). A "FINE" integration grid [15,28] was used throughout this study.
For the chemical-shift calculations, the sum-over-states density-functional perturbation theory (SOS-DFPT) approach was used in its LOC1 approximation [15] with individual gauges for localized orbitals (IGLO) [29]. The exchange-correlation functional of Perdew and Wang (1991) [30] was employed. The same metal ECPs and valence basis sets were used as for the structure optimizations (cf. above), but all electrons on the ligand atoms were included explicitly using IGLO-II basis sets [29]. We employed auxiliary bases of sizes 5,2 (O, C) and 5,1 (H).
The ^{13}C and ^{1}H shifts are given with respect to TMS, and ^{17}O shifts with respect to H_2O^{vap}. The structures of the reference molecules were optimized at the same computational levels as those of the complexes. The computed absolute shieldings of TMS are 187.5 (C) and 31.0 (H) ppm. The oxygen shielding of H_2O is calculated to be 307.3 ppm.
Most calculations were carried out with a modified version of the LCGTO-MCP-DFT program deMon [28]. NBO population analyses [31] were performed with the built-in NBO routines of the Gaussian92/DFT program [32]. These latter calculations involve no fitting of charge density and exchange-correlation potential. They were based on the structures obtained with deMon.

Results

1. Structure Optimizations: A high accuracy of the optimized molecular structures is important for the chemical-shift calculations, as shielding tensors are very sensitive to the structural parameters.[29] Apart from these considerations, the structures are interesting in their own right (not all of them are known experimentally) and will be discussed briefly before turning to the NMR results in the following section.

Calculated and, where available, experimental bond lengths for the Group 4 $[MCp(CO)_4]^-$, the Group 5 $[MCp(CO)_4]$, and the Group 7 $[MCp(CO)_3]$ complexes are summarized in Tables 3, 4, and 5, respectively (the structures for Group 6 $[MCp(CO)_3CH_3]$ species will be discussed in Section 6; see Fig. 1 for the atom labeling). Where experimental data are available (for the Ti,[5a] V,[33a] Nb,[33b] Mn,[33c] and Re[33d] complexes), the calculated distances from the metal to the cyclopentadienyl ligands are found to be slightly too long (by ca. 0.02–0.05 Å for the M···ring centroid separations). If we extrapolate the deviations from experiment to those complexes where no experimental data are available, and keep in mind that the Group 4 species bear one negative charge (and the calculations on the free anions should thus exhibit an additional systematic error due to the neglect of solvation and counterion effects), we can expect that the calculated M–Cp separations for the Zr and Hf complexes are overestimated by approximately 0.06 Å.

  0947-6539/96/0203-0349 $ 15.00+.25/0

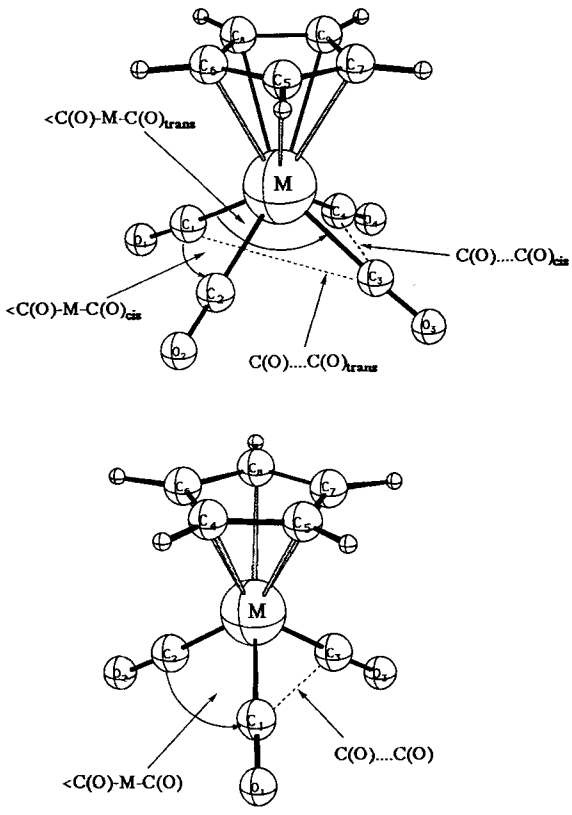

Fig. 1. Definition of internal coordinates and atom labels for piano-stool complexes. Top: $[MCp(CO)_4]$; bottom: $[MCp(CO)_3]$.

For all other bond lengths, the agreement with experiment is better than about 0.02 Å (one very short C–O bond length measured for the Nb complex[33b] is probably unreliable). The variation of the C–C distances within the Cp ligands is calculated to be somewhat smaller than found in the experimental data. C–O bond lengths are very similar for all complexes (slightly greater in the Group 4 anions), as are the C–H bond lengths. Note that for the four-legged complexes the C–H bond that bisects a C(CO)-M-C(CO) angle (C_5–H, cf. Fig. 1, top) is somewhat longer than the other four C–H bonds and slightly bent (by ca. 4°) towards the metal. This suggests agostic interactions which are, however, probably not very strong in view of the experimentally observed low barrier to rotation of the Cp ring relative to the $M(CO)_4$ fragment (as indicated by averaged NMR signals and by disorder in the solid-state structures[5, 33a, b]). Average bond angles agree with experiment to an accuracy of better than about 3 °(only the calculated C(CO)-M-C(CO) angles are given in Tables 3–5).

Metal-to-ligand bond lengths for the Zr and Hf complexes exhibit the expected similarities, as do those for the Nb and Ta species. The most significant structural feature that distinguishes the four-legged from the three-legged piano-stool complexes are the small C-M-C angles for *cis* CO ligands (ca. 72–76° vs. ca. 90–93° in the three-legged species). These small angles will be important in the interpretation of the chemical-shift tensors (see below).

Comparison of quasirelativistic and nonrelativistic ECP results for $[ReCp(CO)_3]$ indicates that scalar relativistic effects contract the M–C(Cp) and M–C(CO) distances by approximately 0.055 and 0.044 Å, respectively. This is consistent with Re–L distances in other complexes.[34a] As the relativistic contraction for the Tc compounds is expected to be much smaller,

Table 3. Calculated (experimental values in parentheses) bond lengths (Å) and bond angles (°) for $[MCp(CO)_4]^-$ (M = Ti, Zr, Hf) [a].

	$[TiCp(CO)_4]^-$	$[ZrCp(CO)_4]^-$	$[HfCp(CO)_4]^-$ (QR) [b]	$[HfCp(CO)_4]^-$ (NR) [c]
M–Cp	2.096 (2.049)	2.265	2.262	2.297
M–C(Cp) [d]	2.403–2.422 (2.356)	2.536–2.582	2.530–2.585	2.563–2.616
M–C_5(Cp)	2.448	2.591	2.583	2.611
M–C(CO) [e]	1.994 (1.996)	2.184	2.182	2.214
C–O [e]	1.180	1.178	1.178	1.177
C–H [d]	1.095	1.095	1.096	1.096
C_5–H	1.107	1.108	1.108	1.109
C–C [f]	1.417–1.427	1.419–1.430	1.419–1.431	1.420–1.430
C(CO)···C(CO)				
cis [g]	2.361	2.645	2.644	2.690
trans [h]	3.339	3.374	3.738	3.804
C(CO)-M-C(CO)				
cis [g]	72.6	74.5	74.6	74.8
trans [h]	113.7	117.8	117.8	118.4

[a] Fully optimized structures; see computational details section. See Figure 1 (top) for internal coordinates and atom labeling. Experimental data for $[TiCp(CO)_4]^-$ from ref. [5a]. Cp = η^5-C_5H_5. [b] Quasirelativistic Hf ECP. [c] Nonrelativistic Hf ECP. [d] Range for carbon atoms 6–9. [e] Average for all carbonyl groups. [f] Range for all C–C bonds. [g] Average for *cis* CO ligands. [h] Average for *trans* CO ligands.

Table 4. Calculated (experimental values in parentheses) bond lengths (Å) and bond angles (°) for $[MCp(CO)_4]$ (M = V, Nb, Ta) [a].

	$[VCp(CO)_4]$	$[NbCp(CO)_4]$	$[TaCp(CO)_4]$
M–Cp	1.932 (1.913)	2.137 (2.084)	2.149
M–C(Cp) [b]	2.247–2.287 (2.226–2.321)	2.438–2.461 (2.377–2.408)	2.438–2.470
M–C_5(Cp)	2.320	2.500	2.517
M–C(CO) [c]	1.914 (1.940)	2.082 (2.096)	2.098
C–O [c]	1.162 (1.145)	1.161 (1.112 [d],1.145)	1.163
C–H [b]	1.094	1.095	1.095
C_5–H	1.106	1.105	1.106
C–C [e]	1.422–1.428 (1.397–1.432)	1.425–1.432 (1.390–1.427)	1.423–1.433
C(CO)···C(CO)			
cis [f]	2.360	2.523	2.554
trans [g]	3.336	3.577	3.615
C(CO)-M-C(CO)			
cis [f]	76.1	74.6	75.0
trans [g]	121.2	117.8	118.9

[a] Fully optimized structures, see computational details section. See Figure 1 (top) for internal coordinates and atom labeling. Experimental data from refs. [33a,b]. Cp = η^5-C_5H_5. [b] Range for carbon atoms 6–9. [c] Average for all carbonyl groups. [d] Value probably wrong, see text. [e] Range for all C–C bonds. [f] Average for *cis* CO ligands. [g] Average for *trans* CO ligands.

Table 5. Calculated (experimental values in parentheses) bond lengths (Å) and bond angles (°) for three-legged piano-stool carbonyl complexes [a].

	$[MnCp(CO)_3]$	$[TcCp(CO)_3]$	$[ReCp(CO)_3]$ (QR)	$[ReCp(CO)_3]$ (NR)
M–Cp	1.799 (1.775)	1.981	2.013 (1.980)	2.079
M–C(Cp) [b]	2.170 (2.149)	2.324	2.355 (2.307)	2.408
M–C(CO) [c]	1.786 (1.808)	1.917	1.932 (1.905)	1.976
C–O [c]	1.163 (1.148)	1.164	1.165 (1.168)	1.162
C–H [b]	1.094	1.094	1.094	1.094
C–C [d]	1.426–1.436 (1.424)	1.427–1.441	1.427–1.441 (1.387–1.443)	1.427–1.436
C(CO)···C(CO) [e]	2.596	2.739	2.781	2.806
C(CO)-M-C(CO) [e]	93.3	91.4	92.1	90.5

[a] Fully optimized structures, see computational details section; Cp = η^5-C_5H_5. See Figure 1 (bottom) for internal coordinates and atom labeling. Experimental data from refs. [33c,d]. [b] Average for all Cp carbon atoms. [c] Average for all carbonyl groups. [d] Range for all C–C bonds. [e] Average for all CO ligands.

0947-6539/96/0203-0350 $ 15.00+.25/0 Chem. Eur. J. 1996, 2, No. 3

relativity accounts partially for the very similar Tc–L and Re–L distances (this also holds true for other 4d/5d comparisons, to a varying degree[34b]). The corresponding relativistic contractions of the metal–ligand distances for $[HfCp(CO)_4]^-$ are somewhat smaller (ca. 0.03 Å, see Table 3) than for the rhenium complex.

2. Isotropic Chemical Shifts: Calculated isotropic carbon, oxygen, and hydrogen chemical shifts are summarized in Table 6. Where available, experimental data are given as well. The overall agreement between calculated and experimental shifts is reasonable, and most of the periodic trends are reproduced faithfully. In particular, the extreme deshielding in the δ ^{13}C(CO) of the four-legged Group 4 piano-stool anions is reproduced by the calculations, as are the lower but still deshielded (ca. $\delta = 250$) values for the Group 5 analogues and the "normal" (ca. $\delta = 190-220$) ^{13}C(CO) shifts for the three-legged Group 7 complexes (see Fig. 2). It is gratifying to see that the calculations do describe these trends correctly. This permits the detailed analysis of factors which lead to the large deshielding (see below).

Table 6. Calculated and experimental ^{13}C, ^{17}O, and ^{1}H isotropic chemical shifts (δ) [a] for piano-stool carbonyl complexes

	δC(CO)		δC(Cp)		δO		δH	
	exp.	calcd [b]	exp.	calcd [b]	exp.	calcd [b]	exp.	calcd [b]
$[TiCp(CO)_4]^-$ [c]	289	275.3	93	96.5		474	5.05	5.4
$[ZrCp(CO)_4]^-$ [c]	292	298.8	98	95.2		541	5.55	5.7
$[HfCp(CO)_4]^-$ [c]	291	301.0	97	96.7		546	5.51	5.7
$[VCp(CO)_4]$ [d]	256.6	242.0	92.5	95.7		435	5.08	5.4
$[NbCp(CO)_4]$ [e]	251.0	250.3	94.7	97.9		469		5.9
$[TaCp(CO)_4]$		253.6		97.2		476		5.9
$[MnCp(CO)_3]$ [f]	220–225	224.4	83.1	91.4	410	384	4.75	5.5
$[TcCp(CO)_3]$		212.0		91.4		364		6.1
$[ReCp(CO)_3]$ [g]	195.0	208.0	84.5–85.9	89.9	346	350	5.37	6.2

[a] Shifts referenced to TMS for carbon and hydrogen, and to H_2O^{vap} for oxygen, with positive sign-more deshielded convention. Experimental ^{17}O data have been converted by adding the experimental gas/liquid shift ($\delta = 36$) of water (R. E. Wasylishen, S. Mooibroek, J. B. Macdonald, *J. Chem. Phys.* **1984**, *81*, 1057). Cp = η^5-C_5H_5. [b] Average values for all C(CO), C(Cp), O(CO), and H(Cp) atoms. [c] Experimental data from ref. [5e]. [d] Experimental data from: D. Rehder, *Inorg. Chim. Acta* **1986**, *111*, L13 and A. N. Nesmeyanov, E. I. Fedin, L. A. Fedorov, P. V. Petrovski, *J. Struct. Chem.* **1972**, *6*, 964. [e] Experimental data from D. Rehder, *Chimia* **1986**, *40*, 186. [f] Experimental data from ref. [1]. [g] Experimental data from I. R. Lyatifov, G. I. Gulieva, V. N. Babin, R. B. Materikova, P. V. Petrovski, E. I. Fedin, *J. Organomet. Chem.* **1987**, *326*, 93.

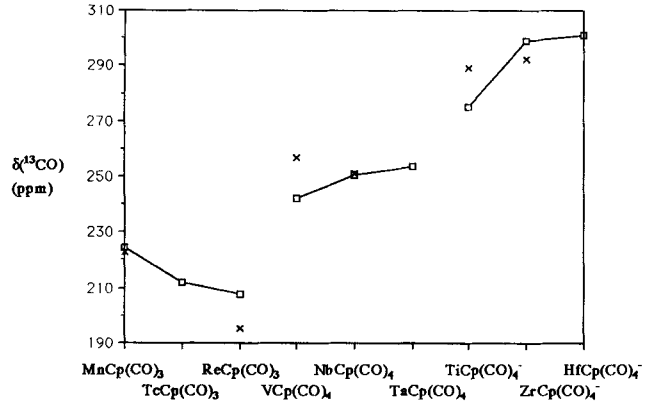

Fig. 2. Comparison of calculated (squares connected by lines) and experimental (crosses) isotropic ^{13}C(CO) NMR shifts in piano-stool carbonyl complexes (cf. Table 6).

Some of the more subtle periodic trends observed within a given triad are not matched exactly by the calculations. This is only partly due to specific errors (electron correlation, neglect of spin–orbit coupling, and errors in the computed structures; see below) in the molecular calculations. A comparison with experimental solution data is also complicated by solvent and counterion effects, which are not taken into account in the present calculations on isolated molecules or anions. Additionally, the observed thermal averaging for similar atoms (for all carbonyl groups and for all carbon or hydrogen atoms in the cyclopentadienyl ligands) was simulated by simply taking the average of the calculated values for these groups of atoms. This is also a potential source of error, as is the neglect of rovibrational corrections.

The calculations underestimate the ^{13}C(CO) shifts for $[TiCp(CO)_4]^-$ and for $[VCp(CO)_4]$ by approximately 12–14 ppm, whereas those for the Hf and Re species are somewhat too large. This is consistent with our previous experience.[16, 18] Extension of the ligand basis sets from IGLO-II to IGLO-III is expected to increase the ^{13}C(CO) shifts by around 5–10 ppm[16, 18] and thus to bring the data for the Ti and V species into good agreement with experiment (the shifts for the Mn complex would thus come out somewhat too large). Basis-set extension would, however, increase the errors for the 5d complexes by a similar amount. We suspect that the overestimation of δ ^{13}C(CO) for the 5d carbonyl complexes is partly due to the neglect of spin–orbit coupling in the calculations.[16, 18] The relatively large computed M–C(Cp) distances for the Zr and Hf complexes (cf. above) may also affect the shifts for these two species. Note that the influence of counterions is also nonnegligible for the Group 4 anions.[5f, 35] The difference between the calculated shift for the Ti anion and those of its Zr and Hf congeners is thus too large (the same holds for the difference between $[VCp(CO)_4]$ and $[NbCp(CO)_4]$), and the shift for the Re complex is somewhat too close to that calculated for its Mn analogue. Interestingly, theory and experiment agree, at least qualitatively, that the shifts decrease down the Group 7 triad (the typical "triad" effect[1, 2, 18]) but not down Group 4.

The calculations predict that the ^{17}O resonances for the Group 4 anions are also at unusually high frequencies, at around $\delta = 500-550$ (vs. H_2O^{vap}). This is a range more typical for shifts of bridging than of terminal carbonyl oxygens.[36] Resonances for the latter are expected[36] at around $\delta = 350-400$, as calculated and observed for the three-legged Group 7 complexes (see Table 6). The four-legged Group 5 species are in an intermediate range of $\delta = 430-480$. Thus, the trends in the ^{13}C(CO) shifts parallel those in the oxygen shifts. This is significant since substituents, which alter the degree of backbonding in transition-metal carbonyl complexes, usually influence the carbon and oxygen shifts in opposite ways.[36] Experimental oxygen shifts are available only for $[MCp(CO)_3]$ (M = Mn, Re). For these two species, the calculated shifts agree well with experiment (Table 6). Calculations for $M(CO)_6$ (M = Cr, Mo, W) at the same basis-set level give very similar accuracy.[18]

The isotropic ^{13}C shifts for the five cyclopentadienyl carbon atoms were averaged to allow comparison with the thermally averaged experimental data. As for the carbonyl carbon shifts, the calculations reproduce the general trends, but deviate from experiment in the more subtle details. Thus, the lower frequencies in the three-legged Group 7 species compared to the four-legged Group 4 and 5 species are predicted correctly by the calculations, whereas some of the smaller fluctuations in the experimental data within a given triad are not reproduced (Table 6). The calculated shifts for the five nonequivalent car-

bon atoms vary by approximately 2–7 ppm for the four-legged and by approximately 11–14 ppm for the three-legged complexes. This is mainly due to the chemical inequivalence of the nuclei in the "clamped" molecular structures employed for the calculations, and to a smaller extent also to numerical (grid) reasons. Thus, we cannot expect better agreement of the averaged shifts with experiment. Low-temperature experiments might resolve the shifts for different carbon sites, provided that the rotation of the cyclopentadienyl ligands can be frozen out.

The calculated ^{1}H shifts show differences of between 0.5 (M = V) and 1.5 ppm (M = Mn) for nonequivalent atoms. Thus, there is some uncertainty connected with the averaged values. Moreover, the ^{1}H shifts are known to be very solvent dependent.[37] Thus, we should not expect the agreement between theory and experiment to be very good. Where experimental data for Group 4 and 5 species is available, the calculated ^{1}H shifts are found to be systematically overestimated by approximately 0.25–0.35 ppm. The deviations are larger (ca. 0.75-0.8 ppm) for the Group 7 complexes.

3. ^{13}C(CO) Shielding Tensors: More information about the origin of the unusually large carbonyl ^{13}C shifts, particularly for the Group 4 complexes, is provided by a detailed examination of the computed shielding tensors (cf. Table 7). The shielding anisotropy $[(\sigma_{11} + \sigma_{22})/2 - \sigma_{33}]$ is particularly striking: While the three-legged Group 7 complexes exhibit anisotropy values in the 400–450 ppm range typical for terminal carbonyl ligands, the anisotropy for the four-legged Group 5 complexes is only around 320–370 ppm, and that for the Group 4 anions is only around 220–300 ppm. The latter results are close to values observed for bridging carbonyl groups.[38] Both with the Group 4 anions and with the Group 5 molecules, the anisotropy for the 4d and 5d species is calculated to be much smaller than that for the corresponding 3d complex. Scalar relativistic effects reduce the shielding anisotropy for $[HfCp(CO)_4]^-$ and $[ReCp(CO)_3]$ slightly (Table 7) but will be neglected in the following discussion.

Table 7. Calculated absolute ^{13}C(CO) shielding tensors (ppm).

	σ_{11}	σ_{22}	σ_{33}	σ_{av}	$(\sigma_{11} + \sigma_{22})/2 - \sigma_{33}$
$[TiCp(CO)_4]^-$	−198.5	−171.1	106.4	−87.6	−291.2
$[ZrCp(CO)_4]^-$	−195.5	−179.5	41.0	−111.3	−228.5
$[HfCp(CO)_4]^-$					
QR//QR [a]	−191.3	−176.5	27.5	−113.5	−211.4
NR//QR [b]	−196.0	−180.9	46.8	−110.1	−235.3
NR//NR [c]	−196.3	−182.0	37.8	−113.5	−227.0
$[VCp(CO)_4]$	−183.0	−171.1	192.5	−53.9	−369.6
$[NbCp(CO)_4]$	−179.7	−167.0	163.9	−60.9	−337.3
$[TaCp(CO)_4]$	−177.5	−165.1	148.0	−64.9	−319.9
$[MnCp(CO)_3]$	−183.6	−182.4	252.4	−37.9	−435.4
$[TcCp(CO)_3]$	−166.1	−163.7	256.4	−24.5	−421.3
$[ReCp(CO)_3]$					
QR//QR [a]	−156.5	−155.7	254.8	−19.1	−410.9
NR//QR [b]	−164.8	−164.5	257.1	−24.1	−421.8
NR//NR [c]	−168.6	−165.5	258.5	−25.2	−425.6

[a] Quasirelativistic ECP both in shift calculation and in structure optmization. [b] Nonrelativistic ECP in shift calculation at quasirelativistically optimized structure. [c] Nonrelativistic ECP both in shift calculation and in structure optmization.

The above results indicate remarkable deviations in the electronic structure of the carbonyl moieties in the four-legged complexes from that typical for terminal carbonyl ligands. Inspection of the individual shielding tensor elements (Table 7) indicates that the tensors still have approximately axial symmetry, with relatively unremarkable perpendicular components (σ_{22} is slightly less negative than σ_{11}). However, σ_{33}, which is oriented roughly parallel to the M-C-O direction, is considerably reduced compared to those for the three-legged Group 7 complexes or for normal octahedrally coordinated species.[18, 38, 39] For free CO (which for symmetry reasons has no paramagnetic contributions to σ_{33}[40]), σ_{33} is 274 ppm at this computational level.[18] This may be taken roughly as the "diamagnetic limit". Thus, there are appreciable paramagnetic contributions to the parallel tensor element in the four-legged carbonyl complexes, particularly for the Group 4 species.

Further information may be obtained by breaking the tensor elements down into contributions from the individual localized molecular orbitals (LMOs) employed in the IGLO procedure.[29] Results for two four-legged complexes (M = Ti, Zr), and for comparison for two three-legged complexes (M = Mn, Tc), are shown in Table 8. Contributions from predominantly ligand-centered orbitals (the carbon 1s AO, the C(CO)–M σ-bonding LMO, the oxygen lone-pair, and the three C–O bonding LMOs) are listed separately from those with mainly metal $(n-1)$p and $(n-1)$d character. Among the first set of LMOs, the contributions from the C–O triple-bonding orbitals to σ_{33} are somewhat larger (i.e., more diamagnetic) in the four-legged species than in the three-legged (or other "normal") systems.[18] The contributions from the oxygen lone pair and from the C–M bond do not differ very much in the four complexes (except for the slight metal-dependent variations in the σ-C–M LMO contributions[18]). Strikingly large paramagnetic contributions to σ_{33} in the four-legged Group 4 anions come from the two LMOs resembling metal d orbitals (d_{z^2} and d_{xy}[19]). Without these contributions, the ^{13}C(CO) shielding tensors for $[TiCp(CO)_4]^-$ and $[ZrCp(CO)_4]^-$ would look very much like those for "normal" terminal carbonyl groups, with an anisotropy of approximately 450 ppm and σ_{33} elements close to the above-mentioned "diamagnetic limit" of around 270–280 ppm (cf. rows "$\sum$ excluding p,d(M)" in Table 8). These metal-centered LMOs contribute a smaller yet significant share to σ_{11} and σ_{22} elements. The slightly larger d_{xy} LMO contribution to σ_{11} compared to the d_{z^2} LMO contribution to σ_{22} partly accounts for the deviation of the shielding tensors from axial symmetry. Overall, the metal d-orbital contributions account for a dramatic decrease of the isotropic ^{13}C shielding by ca. 125 and ca. 90 ppm for the Zr and Ti complexes, respectively (there are also smaller, nonnegligible contributions from metal semicore $(n-1)$p orbitals, see Table 8).

The contributions from LMOs resembling metal d orbitals (ca. −20 to −30 ppm for σ_{av}) are much smaller in the three-legged Group 7 complexes. They are similar for all three tensor components and thus do not affect the shift anisotropy very much (Table 8). The analysis for $[MnCp(CO)_3]$ and $[TcCp(CO)_3]$ therefore gives very similar results to those found for the Group 6 hexacarbonyl compounds,[18] albeit with slightly larger contributions from metal-centered orbitals. We have not given detailed analyses for the Hf and Re systems, as the results are very similar to those for the Zr and Tc species, respectively. The Group 5 compounds show similar contributions from metal d orbitals to the Group 4 anions, but on a smaller scale (ca. −60 to −95 ppm for σ_{33}; ca. −30 to −50 ppm for σ_{av}).

A similar decomposition into contributions from canonical Kohn–Sham (KS) orbitals instead of localized MOs can also be achieved by performing calculations with a common gauge origin (e.g., at the nucleus of interest[18]). We will not give the results for this type of analysis (which depends on whether the shifts obtained with common gauge origin exhibit the correct trends) in detail, but would like to point out that the two highest occupied canonical MOs in the four-legged complexes are related to

0947-6539/96/0203-0352 $ 15.00+.25/0 Chem. Eur. J. 1996, 2, No. 3

Table 8. LMO decomposition of carbon shielding tensors [a].

LMO	[TiCp(CO)$_4$]				[ZrCp(CO)$_4$]			
	σ_{11}	σ_{22}	σ_{33}	σ_{av}	σ_{11}	σ_{22}	σ_{33}	σ_{av}
1s(C_1)	200.0	200.0	200.0	200.0	200.0	200.0	200.0	200.0
Bd(M–C_1)	−209.0	−180.4	23.0	−122.1	−198.5	−179.8	22.6	−118.5
LP(O_1)	−53.0	−55.3	3.2	−35.0	−54.3	−55.9	3.2	−35.7
3 × Bd(C_1≡O_1)	−83.6	−96.6	80.6	−33.2	−87.4	−96.6	90.8	−31.1
Σ excluding p,d(M) [b]	−143.1	−129.8	309.3	12.2	−137.7	−129.8	319.2	17.2
d_{xy}(M) [c]	−54.1	2.5	−121.0	−57.5	−56.4	0.9	−148.2	−67.9
d_{z^2}(M) [c]	2.6	−30.5	−71.7	−33.2	2.9	−39.1	−110.0	−48.7
Σ(n−1)p [d]	−5.4	−6.1	0.1	−3.8	−5.9	−8.0	−10.1	−8.0
Σ [e]	−200.0	−163.9	116.7	−82.3	−197.1	−176.0	50.9	−107.4
total [f]	−199.8	−173.0	110.2	−87.5	−197.9	−182.6	42.8	−112.6
LMO	[MnCp(CO)$_3$]				[TcCp(CO)$_3$]			
	σ_{11}	σ_{22}	σ_{33}	σ_{av}	σ_{11}	σ_{22}	σ_{33}	σ_{av}
1s(C_1)	200.0	200.0	200.0	200.0	200.0	200.0	200.0	200.0
Bd(M–C_1)	−201.6	−204.8	23.1	−127.8	−192.7	−189.3	22.8	−119.7
LP(O_1)	−55.2	−52.4	3.3	−34.8	−49.6	−52.8	3.4	−33.0
3 × Bd(C_1≡O_1)	−88.0	−86.5	49.2	−41.8	−83.1	−88.3	50.2	−40.4
Σ excluding p,d(M) [b]	−144.8	−143.7	275.6	−4.4	−125.4	−130.4	276.4	6.9
Σ(n−1)d(M) [c]	−33.6	−34.0	−27.2	−31.5	−33.7	−23.1	−14.8	−23.8
Σ(n−1)p(M) [d]	−4.0	−9.7	−0.5	−4.8	−9.7	−10.4	−7.0	−8.7
Σ [e]	−182.4	−187.3	247.8	−40.7	−167.8	−163.9	254.6	−25.6
total [f]	−183.6	−182.4	252.4	−37.9	−166.1	−163.7	256.4	−24.5

[a] Absolute shieldings in ppm. Only LMOs with at least one individual contribution > 3 ppm have been included. [b] All contributions except LMOs resembling metal (n−1)p and d AOs. [c] Contributions from LMOs resembling metal d AOs. [d] Sum of contributions from LMOs resembling (n−1)p AOs. [e] Sum of all listed contributions. [f] Sum of all contributions.

the metal d_{xy}- and d_{z^2}-like LMOs discussed above. Their contributions to the shielding tensors behave very similar to those of the corresponding LMOs. Further decomposition into individual electronic "excitations" (i.e., occupied–virtual KS orbital combinations)[18] shows that many different transitions contribute. The overall trend in the energy separation of these two highest occupied MOs from the virtual MO manifold is [HfCp(CO)$_4$]$^-$ ≈ [ZrCp(CO)$_4$]$^-$ > [TiCp(CO)$_4$]$^-$ ≫ [TaCp(CO)$_4$] ≈[NbCp(CO)$_4$]>[VCp(CO)$_4$], consistent with the shielding trends.

4. ^{17}O Shielding Tensors: In view of the unusually large isotropic oxygen shifts found in the calculations for the four-legged carbonyl complexes (Section 2, Table 6), it is interesting to have a closer look at the oxygen shielding tensors as well (Table 9). In a similar manner as discussed above for the ^{13}C(CO) tensors, the shielding anisotropy gives the clearest indication for unusual ^{17}O shielding tensors in the four-legged species, particularly for the Group 4 anions. Thus, while the three-legged Group 7 carbonyls exhibit "normal"[18, 36, 39] anisotropy values for terminal carbonyl ligands of around −500 to −600 ppm, those for [MCp(CO)$_4$] (M = Nb, Ta) are around −350 to −400 ppm, and those for [MCp(CO)$_4$]$^-$ (M = Zr, Hf) are only around −125 to −170 ppm. This means, the reduction in the anisotropy of the oxygen shielding tensors is even more dramatic than for the carbon shielding tensors (cf. above). The Ti and V complexes have a more negative anisotropy than their heavier congeners, but still much less so than the "normal" Group 7 complexes. No carbonyl oxygen shift tensors for bridging ligands have been determined experimentally yet. Our own preliminary computational results indicate that a similar reduction in the shielding anisotropy as found here for the Group 4 piano-stool carbonyl complexes also takes place for bridging as compared to "normal" terminal carbonyl oxygen.[41]

Table 9. Calculated absolute oxygen shielding tensors (ppm).

	σ_{11}	σ_{22}	σ_{33}	σ_{av}	$(\sigma_{11}+\sigma_{22})/2-\sigma_{33}$
[TiCp(CO)$_4$]$^-$	−268	−264	+31	−167	−297
[ZrCp(CO)$_4$]$^-$	−296	−289	−123	−236	−169
[HfCp(CO)$_4$]$^-$	−285	−275	−154	−238	−126
[VCp(CO)$_4$]	−304	−291	+189	−135	−486
[NbCp(CO)$_4$]	−311	−295	+92	−171	−394
[TaCp(CO)$_4$]	−302	−280	+49	−177	−340
[MnCp(CO)$_3$]	−330	−280	+360	−83	−665
[TcCp(CO)$_3$]	−291	−244	+345	−63	−613
[ReCp(CO)$_3$]	−261	−216	+329	−50	−507

As for the carbon shielding tensors (see above), the low σ_{33} elements (Table 9) account for the small anisotropy of the oxygen shielding tensors, and for the unusually large isotropic shifts (cf. Table 6), whereas the σ_{11} and σ_{22} elements are comparable for the three-legged d^6 and four-legged d^4 systems (the "diamagnetic limit" σ_{33} value for free CO is ca. 415 ppm at this level[18]). An LMO decomposition of the shielding tensors for the Ti, Zr, Mn, and Tc species (Table 10) reveals a similar but not identical situation as for the ^{13}C(CO) tensors. In addition to large contributions from the metal d type LMOs for the former two systems, considerable paramagnetic parts of σ_{33} are also due to the C≡O bonds. This suggests a significant distortion of the C–O bond compared to "normal" bonding situations (see below). A similar situation with respect to LMO contributions from the C–O bonds holds in bridging carbonyl ligands, that is, more positive contributions to σ_{33} of the carbon shielding tensors (as in Table 8) but significant negative contributions to the oxygen σ_{33} (Table 10).[41] The decomposition into LMO contributions may have reached the limit of its usefulness in this

Table 10. LMO decomposition of oxygen shielding tensors [a].

LMO	$[TiCp(CO)_4]$				$[ZrCp(CO)_4]$			
	σ_{11}	σ_{22}	σ_{33}	σ_{av}	σ_{11}	σ_{22}	σ_{33}	σ_{av}
$1s(O_1)$	270.1	270.1	270.1	270.1	270.1	270.1	270.1	270.1
$Bd(M-C_1)$	−116.3	−120.7	1.9	−78.4	−119.6	−120.8	−1.2	−80.5
$LP(O_1)$	−150.1	−129.6	27.5	−84.1	−161.8	−132.2	23.0	−90.3
$3\times Bd(C_1\equiv O_1)$	−232.3	−235.3	−69.0	−164.8	−237.5	−238.8	−109.0	−195.2
$\sum$ excluding p,d(M) [b]	−228.6	−215.5	230.3	−71.4	−248.8	−221.7	183.0	−95.9
d_{xy}(M) [c]	−8.2	−39.1	−119.3	−55.6	−2.3	−53.3	−174.1	−76.5
d_{z^2}(M) [c]	−18.2	−4.5	−69.6	−30.7	−32.0	−11.5	−119.2	−54.2
$\sum(n-1)$p(M) [d]	−6.0	−3.0	−3.7	−4.2	−5.7	−5.0	−13.4	−8.0
$\sum$ [e]	−261.0	−262.1	36.7	−161.9	−288.8	−291.5	−123.8	−234.6
total [f]	−268.2	−264.0	31.3	−167.0	−296.4	−289.1	−123.1	−236.2
LMO	$[MnCp(CO)_3]$				$[TcCp(CO)_3]$			
	σ_{11}	σ_{22}	σ_{33}	σ_{av}	σ_{11}	σ_{22}	σ_{33}	σ_{av}
$1s(O_1)$	270.1	270.1	270.1	270.1	270.1	270.1	270.1	270.1
$Bd(M-C_1)$	−118.1	−118.4	2.9	−77.8	−112.2	−111.4	2.9	−73.5
$LP(O_1)$	−170.7	−152.0	34.7	−96.0	−158.7	−137.5	34.6	−87.2
$3\times Bd(C_1\equiv O_1)$	−268.0	−246.3	74.0	−146.8	−254.5	−236.9	67.6	−141.3
$\sum$ excluding p,d(M) [b]	−286.7	−246.6	381.8	−50.5	−255.3	−215.7	375.2	−31.9
$\sum(n-1)$d(M) [c]	−33.7	−29.1	−20.5	−27.6	−22.8	−24.6	−22.1	−23.1
$\sum(n-1)$p(M) [d]	−6.1	−5.4	−2.4	−4.6	−10.4	−6.4	−8.9	−8.6
$\sum$ [e]	−328.0	−281.1	359.5	−82.7	−288.5	−246.7	344.2	−63.6
total [f]	−330.0	−279.9	359.6	−83.4	−291.2	−244.1	345.0	−63.4

[a] Absolute shieldings in ppm. Only LMOs with at least one individual contribution >5 ppm have been included. [b] All contributions except LMOs resembling metal $(n-1)$p and d AOs. [c] LMOs resembling metal d AOs. [d] LMOs resembling metal $(n-1)$p AOs. [e] Sum of all listed contributions. [f] Sum of all contributions.

context, as the metal d orbitals and the M–C and C–O antibonding orbitals mix extensively (i.e., the corresponding LMOs have significant tails at other centers; see below).

5. Bonding Analyses: The results obtained above from LMO decomposition of the carbonyl shielding tensors fit nicely with previous qualitative MO pictures (based on extended Hückel calculations) for four-legged piano-stool carbonyl complexes.[19–21] The work of Kubáček, Hoffmann, and Havlas[19] is fundamental in this respect. In particular, the d_{xy}- and d_{z^2}-like orbitals, which are so important for the unusually large NMR shifts of the carbonyl ligands, also feature as the two highest occupied MOs in extended Hückel calculations (cf. Fig. 3). Delocalization of these orbitals through backbonding into the carbonyl π-antibonding MOs has been discussed in detail.[19]

As a further illustration, natural bond orbital (NBO)[31] analyses have been carried out, based on the Kohn–Sham calcu-

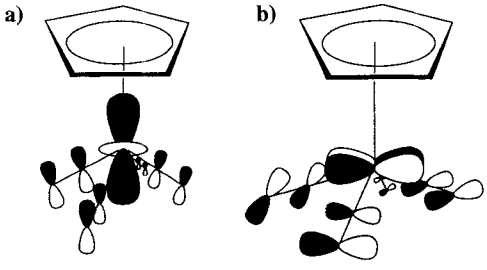

Fig. 3. Schematic picture of occupied metal d orbitals in d^4 $[MCp(CO)_4]$. a) $(s)d_{z^2}$; b) d_{xy} (cf. refs. [19,20]).

Table 11. Results of NBO analyses for four-legged piano-stool complexes $[MCp(CO)_4]^-$ (M = Ti, Zr, Hf) and $[MCp(CO)_4]$ (M = V, Nb, Ta) [a].

	Ti	Zr	Hf	V	Nb	Ta
NPA						
Q(M)	−0.697	−0.157	+0.151	−0.909	−0.398	−0.103
s(M)	0.365	0.357	0.391	0.381	0.370	0.422
p(M)	0.017	0.018	0.014	0.015	0.015	0.012
d(M)	4.364	3.836	3.464	5.555	5.065	4.693
Q(CO)	+0.007	−0.100	−0.160	+0.210	+0.121	+0.061
Q(C) [b]	+0.518	+0.404	+0.345	+0.636	+0.540	+0.478
Q(O)	−0.511	−0.504	−0.505	−0.426	−0.419	−0.417
$Q[M(CO)_4]$	−0.667	−0.552	−0.486	−0.068	+0.088	+0.143
Q(Cp)	−0.333	−0.448	−0.514	+0.068	−0.088	−0.143
NBO $[sd_{z^2}(M)]$ [c]						
% s	29	18	14	45	29	22
% d	71	82	86	55	71	78
NLMO $[d_{xy}(M)]$ [d]						
% M	48.9	48.0	43.8	64.5	61.6	56.9
% C [b]	9.4	9.4	10.1	6.3	6.7	7.5
% O	3.0	3.1	3.3	2.1	2.3	2.7
NLMO $[sd_{z^2}(M)]$ [d]						
% M	47.2	46.8	42.9	60.2	57.7	53.8
% C [b]	9.8	9.9	10.6	7.0	7.8	8.5
% O	3.0	3.2	3.5	2.2	2.4	2.8
NLMO [d] (Bd M–CO [e])						
% M	28.4	22.7	21.2	35.1	30.0	28.6
% C [b]	67.9	75.6	77.1	61.3	67.9	69.4

[a] Based on KS calculations (Becke–Perdew functionals) with quasirelativistic ECPs and basis sets as employed for the structure optimizations (see computational details section). Q(X) = partial charge; s,p,d(X) = metal valence populations. [b] Carbonyl carbon. [c] Metal contributions to natural bond orbital. [d] Composition of natural localized MO. [e] M–C σ bond.

0947-6539/96/0203-0354 $ 15.00+.25/0 Chem. Eur. J. 1996, 2, No. 3

lations. Table 11 summarizes partial charges, metal valence populations, and compositions of natural localized orbitals (NLMOs) and NBOs for the four-legged piano-stool complexes considered. The NPA charges[31] on the carbonyl ligands, Q(CO), are very instructive. They vary from appreciably negative to appreciably positive along the series $[HfCp(CO)_4]^- < [ZrCp(CO)_4]^- < [TiCp(CO)_4]^- < [TaCp(CO)_4] < [NbCp(CO)_4] < [VCp(CO)_4]$; this is consistent with the expected decrease in the backbonding properties of the metal centers. The metal d population increases considerably along the same series. These changes within the $M(CO)_4$ fragment obviously influence the charges on the cyclopentadienyl ligands as well. The change in total charge from the Group 4 anions to the Group 5 neutral systems has to be kept in mind, however.

The strictly localized natural bond orbital (NBO) with predominantly metal d_{z^2} character (see Fig. 3a) has some s contributions as well (Table 11). These decrease down a given triad and are larger for the Group 5 than for the Group 4 complexes. NLMOs may be constructed from this NBO and from the one corresponding to the metal d_{xy} orbital (Fig. 3b) by allowing delocalization tails on other centers to be formed. The coefficients of these NLMOs on the carbonyl carbon and oxygen atoms are appreciable and decrease along the series $[HfCp(CO)_4]^- > [ZrCp(CO)_4]^- > [TiCp(CO)_4]^- > [TaCp(CO)_4] > [NbCp(CO)_4] > [VCp(CO)_4]$ (Table 11). This further corroborates the backbonding trends discussed above.

6. The Complexes $[MCp(CO)_3CH_3]$ (M = Cr, Mo, W): Mann[42] found that $[WCp(CO)_3CH_3]$ does not follow the correlation (δ ^{13}C is much too high) between ^{13}C(CO) shifts and CO stretching force constants that holds for a series of $[W(CO)_nL_{6-n}]$ d^6 complexes. The carbonyl shifts for this four-legged piano-stool d^4 complex (see Fig. 4) are not as dramatically large as for some complexes discussed above. Nevertheless, Mann's findings[42] suggest that metal d-orbital contributions may also strongly influence the shielding tensors in Group 6 d^4 species. To verify this hypothesis, ECP/SOS-DF-PT(IGLO) calculations were carried out on $[MCp(CO)_3CH_3]$ (M = Cr, Mo, W). The presence of a methyl group instead of one CO "leg" in the piano stool gives rise to two different CO environments, with two CO groups "*cis*" and the third "diagonal" to the methyl group (see Fig. 4). It is interesting to see how the calculations reproduce the differences in shielding between the different ligand nuclei.

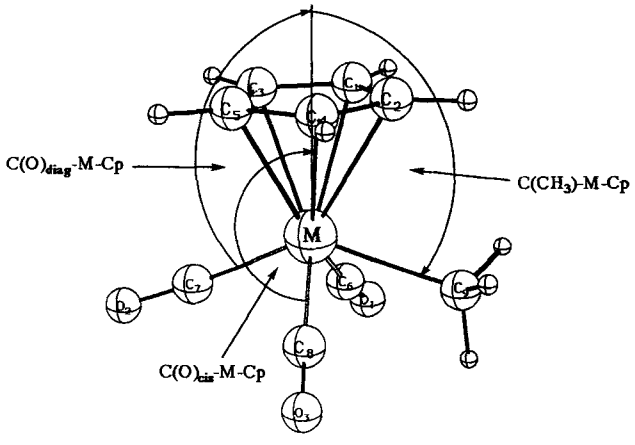

Fig. 4. Definition of internal coordinates and atom labels for $[MCp(CO)_3CH_3]$ (M = Cr, Mo, W).

Results of the structure optimizations are given in Table 12. No experimental structures are known for these species, but the calculations are in good agreement with the structural parameters found for related, substituted complexes.[20,43] In particular, the angles between the methyl group or the "diagonal" CO ligand and the Cp ring midpoint (Fig. 4) are smaller than those for the "*cis*" CO ligands, in agreement with experience and with arguments based on σ- and π-bonding contributions.[20] This leads to angles between *cis* and "diagonal" CO ligands of roughly 80°, and between *cis* CO ligands and the CH_3 group of around 72°.

Table 12. Calculated bond lengths (Å) and bond angles (°) for $[MCp(CO)_3CH_3]$ (M = Cr, Mo, W) [a].

	M = Cr	M = Mo	M = W
M–Cp	1.861	2.045	2.061
M–C(Cp) [b]	2.194–2.258	2.355–2.406	2.369–2.424
M–C(CO)			
cis [c]	1.827	1.978	2.003
diag. [d]	1.823	1.982	2.013
M–C(CH_3)	2.250	2.339	2.345
C–O			
cis [c]	1.162	1.162	1.164
diag. [d]	1.163	1.162	1.163
C(CH_3)-M-Cp	112.0	109.3	107.4
C(CO)-M-Cp			
cis [c]	124.7	126.5	125.7
diag. [d]	118.6	114.7	114.7

[a] Fully optimized structures, see computational details section. See Figure 4 for a definition of the internal coordinates. Cp = η^5-C_5H_5. [b] Range for all C(Cp). [c] Average value for carbonyl ligands *cis* to the methyl group. [d] Carbonyl ligand "diagonal" to the methyl group.

Table 13 gives the ^{13}CO shielding tensors and compares experimental and calculated chemical shifts for the Mo and W complexes. Agreement with experiment is good, comparable to our results for $Mo(CO)_6$ and $W(CO)_6$[18] (the shifts for the tungsten complex are ca. 8–10 ppm too large). The larger deshielding found for the "diagonal" CO ligand is also reproduced faithfully by the calculations. The absolute shielding anisotropy for these more deshielded "diagonal" CO carbon nuclei is consistently smaller than for the less deshielded "*cis*" ligands. For the Mo and W complexes, the anisotropy values are considerably reduced compared to the typical value of around 400 ppm for terminal carbonyl complexes, but not to the same extent as for the Group 4 anions (cf. Table 7). As expected from

Table 13. Calculated absolute ^{13}CO shielding tensors (ppm) in $[MCp(CO)_3CH_3]$ (M = Cr, Mo, W) and comparison of calculated and experimental isotropic shifts.

M		σ_{11}	σ_{22}	σ_{33}	σ_{av}	$(\sigma_{11}+\sigma_{22})/2-\sigma_{33}$	δ_{av}^{calcd} [a]	δ_{av}^{exp} [a]
Cr	*cis* [b]	−186.2	−168.8	239.0	−38.7	−416.5	226.2	
	diag.	−179.0	−170.9	216.4	−44.5	−391.4	232.0	
Mo	*cis* [b]	−176.9	−161.0	230.2	−35.9	−399.2	223.4	226.1 [c]
	diag.	−172.1	−170.6	197.2	−48.5	−368.6	236.0	239.2 [c]
W	*cis* [b]	−173.2	−155.4	216.1	−37.5	−380.4	225.0	215.5 [c]
	diag.	−168.4	−169.2	184.1	−49.2	−349.9	236.7	228.6 [c]

[a] Versus TMS. [b] Average value for both *cis* CO ligands. [c] L. J. Todd, J. R. Wilkinson, *J. Organomet. Chem.* **1978**, *154*, 151.

the previous discussion, the reduced anisotropy is due to low σ_{33} values (Table 13). Similar trends are again found for the oxygen shielding tensors: the "diagonal" CO ligands exhibit lower σ_{33}, and thus larger isotropic shifts and a lower absolute anisotropy (Table 14).

Table 14. Calculated absolute oxygen shielding tensors (ppm) in $[MCp(CO)_3CH_3]$ (M = Cr, Mo, W).

M		σ_{11}	σ_{22}	σ_{33}	σ_{av}	$(\sigma_{11}+\sigma_{22})/2-\sigma_{33}$
Cr	*cis* [a]	−291.8	−248.0	287.5	−84.1	−557.4
	diag.	−305.3	−268.5	271.8	−100.6	−558.7
Mo	*cis* [a]	−268.2	−254.1	253.4	−89.6	−514.6
	diag.	−326.6	−243.9	197.7	−124.3	−483.0
W	*cis* [a]	−251.1	−242.8	219.1	−91.6	−466.1
	diag.	−319.0	−220.1	162.9	−125.4	−432.5

[a] Average value for both *cis* CO ligands.

LMO decomposition of the shielding tensors shows very similar trends in deshielding d-orbital contributions (mainly to σ_{33}) as discussed above for the Group 4 and Group 5 species, but on a much smaller scale. There are nonnegligible $(n-1)$p-orbital contributions suggesting that these semi-core orbitals are also polarized. Both $(n-1)$d- and $(n-1)$p-orbital contributions are larger for the "diagonal" than for the "*cis*" ligands. As a result of less deshielded σ_{11} and σ_{22} but more deshielded σ_{33} compared to $[MCp(CO)_3]$ (M = Mn, Tc, Re), the isotropic shifts for the Group 6 d^4 species are only slightly larger than for the Group 7 d^6 ones (cf. Tables 6 and 13). Only the shielding tensor elements and the small anisotropy in this case reveal the peculiar electronic structure of the four-legged piano-stool complexes.

The methyl groups exhibit decreasing ^{13}C shifts down the group ($\delta_{av}^{calcd} = +5.5$, -2.5, and -4.2 for $[CrCp(CO)_3CH_3]$, $[MoCp(CO)_3CH_3]$, and $[WCp(CO)_3CH_3]$, respectively). The calculated values are larger than the measured ones, which are -22.1 and -34.6 for M = Mo, W, respectively.[44]

7. Bent-Sandwich Complex $[ZrCp_2(CO)_2]$: Since some bent-sandwich d^2 carbonyl complexes of Ti, Zr, and Hf also exhibit unusually large terminal $^{13}C(CO)$ shifts (see Table 1), one of the simplest of these, $[ZrCp_2(CO)_2]$, was also included in our investigation. In this case, the structural parameters obtained from X-ray diffraction were used.[45]

The carbonyl carbon and oxygen shielding tensors, and the corresponding contributions from the single metal d orbital type LMO (see Fig. 5) are given in Table 15. The calculated isotropic $^{13}C(CO)$ shift of $\delta = 263$ agrees well with the experimental value[8] of 265. The absolute values for the anisotropy of both carbon and oxygen shielding tensors are very low. The low σ_{33} of around 120 ppm for the carbon shielding is similar to the

Table 15. Calculated absolute carbonyl carbon and oxygen shielding tensors (ppm) in $[ZrCp_2(CO)_2]$.

		σ_{11}	σ_{22}	σ_{33}	σ_{av}	$(\sigma_{11}+\sigma_{22})/2-\sigma_{33}$
^{13}C	total	−196.5	−151.4	120.6	−75.8	−294.6
	"d_{y^2}" [a]	−53.8	−2.0	−172.0	−75.9	
^{17}O	total	−341.1	−260.0	39.1	−187.3	−339.6
	"d_{y^2}" [a]	−7.3	−43.2	−184.4	−78.3	

[a] Contribution from the LMO resembling the metal d AO (cf. Fig. 5).

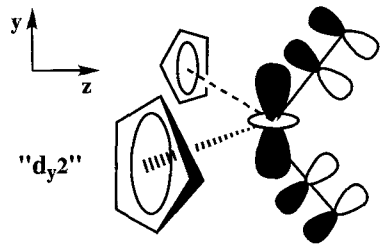

Fig. 5. Schematic picture of occupied metal d orbital in d^2 $[MCp_2(CO)_2]$ (cf. ref. [46]).

results for $[TiCp(CO)_4]^-$ or for $[TaCp(CO)_4]$ (cf. Table 7), that is, much lower than the "diamagnetic limit" of around 270–280 ppm expected for a terminal carbonyl group[18, 38, 39] (see above). The low σ_{33} for the oxygen shielding also compares well to those for the above two complexes (cf. Table 9).

One occupied d orbital has to be considered for this d^2 complex. It may be identified with the orbital shown schematically in Figure 5, in agreement with the results of previous MO studies.[46] In the axis system shown, it is best described as a d_{y^2} orbital.[46] The overlap with the C–O antibonding orbitals and the small angles to the M-C-O axes are apparent in Figure 5, in a similar manner to that discussed for the d orbitals in the four-legged piano-stool complexes (see above and Fig. 3). There is only one instead of two occupied d orbitals as in the piano-stool d^4 examples described above. However, the paramagnetic contributions from this orbital to the carbon and oxygen shieldings (particularly to σ_{33}) are very large (Table 15), placing the shielding tensors for this sandwich complex between those of the Group 4 and Group 5 piano-stool complexes (cf. Tables 7 and 14). Substitution of one CO ligand by a stronger donor but weaker acceptor ligand like $P(OMe)_3$[9a] or PMe_3[10a] obviously expands and polarizes this d orbital and thereby increases its influence even more (Table 1).

8. The Anions $[M(CO)_6]^{2-}$ (M = Ti, Zr, Hf): The octahedral anions $[M(CO)_6]^{2-}$ (M = Ti, Zr, Hf) have even more reduced metal centers than the monoanions $[MCp(CO)_4]^-$. Nevertheless, Ellis et al. found their ^{13}C resonances to be rather unremarkable, in the $\delta = 240-250$ range.[13] Table 16 shows the computational results for the carbon and oxygen shielding tensors in the isolated dianions (using the experimental structures[13]). The calculated isotropic carbon shifts ($\delta = 227$, 219, and 210 for M = Ti, Zr, Hf, respectively) are even lower than the experimental values, increasingly so for the heavier metals. The calculations suggest the presence of the typical "triad effect", that is, a decrease of the ^{13}C shift from Ti to Hf; this shift is absent in the experimental data.[13] Possibly, solvent or counterion effects for these highly charged anions account for the discrepancies between calculation and experiment. In any case, the calculations confirm that these species have shifts in a "normal" range, in contrast to the four-legged Group 4 piano-stool anions.

Moreover, the σ_{33} values and the anisotropy of the shielding tensors are close to "typical" values for terminal CO ligands (Table 16). The anions feature a very high-lying t_{2g} set of occupied d orbitals with a small gap to the lowest-lying virtual orbitals. This is consistent with the observed deep red or violet colors,[13] which are similar to those of the piano-stool Group 4 species.[5e] LMO decomposition of the shielding tensors indicates contributions from metal $(n-1)$p and d orbitals that are roughly twice as large as those for the neutral, isoelectronic complexes $M(CO)_6$ (M = Cr, Mo, W).[18] Thus, for example,

0947-6539/96/0203-0356 $ 15.00+.25/0 Chem. Eur. J. 1996, 2, No. 3

Table 16. Calculated chemical shielding tensors and isotropic shifts [a] for $[M(CO)_6]^{-2}$ (M = Ti, Zr, Hf) (ppm).

		$\sigma_\perp$	$\sigma_\parallel$	σ_{av}	$\sigma_\perp - \sigma_\parallel$	δ_{av}^{calcd}	δ_{av}^{exp} [b]
^{13}C	Ti	−167	215	−40	−382	227	246
	Zr	−155	215	−31	−370	219	245
	Hf	−150	219	−27	−369	214	244
^{17}O	Ti	−213	281	−47	−494	354	
	Zr	−203	281	−42	−484	349	
	Hf	−217	277	−52	−494	359	

[a] ^{13}C shifts vs. TMS, ^{17}O shifts vs. H_2O^{vap}. [b] Ref. [13].

the sum of the metal d-orbital contributions to the isotropic carbon shielding in $[Hf(CO)_6]^{2-}$ is ca. −25 ppm compared to ca. −13 ppm for $W(CO)_6$.[18] However, compared to the d-orbital influences discussed above for the four-legged piano-stool complexes or for $[ZrCp_2(CO)_2]$ (Tables 8, 15), these contributions are small, and the anisotropy of the shielding tensors is not affected much by them.

Discussion

From the above results two conditions may be derived for the occurence of unusually large ^{13}C and ^{17}O shifts and of small shielding anisotropy values in terminal carbonyl ligands: 1) the presence of energetically high-lying and spatially extended occupied metal d orbitals; 2) a favorable spatial arrangement of these d orbitals with respect to the M-C-O axis is needed to allow large contributions to σ_{33}.

The fact that 1) is a necessary condition may be seen easily by comparing the shifts for the Group 4, 5, and 6 examples of four-legged piano-stool complexes (cf. Tables 7, 9, 13, 14). In going from Group 4 to Group 5 to Group 6, the metal d shells of these d^4 complexes become stabilized and contracted (of course one also has to consider the negative charge for the Group 4 species), and the paramagnetic d-orbital contributions to the carbon and oxygen shifts (and thus the total shifts themselves) decrease. Obviously, the donor capability of the ligands also influences the size, shape, and energy of the nonbonding d orbitals. This is apparent, for example, from the differences between "*cis*" and "diagonal" CO ligands in $[MCp(CO)_3CH_3]$ (M = Cr, Mo, W; see Tables 13, 14).

However, condition 2) must also apply. The best example for this is given by the dianions $[M(CO)_6]^{2-}$ (M = Ti, Zr, Hf). In spite of their high-lying, spatially extended set of d orbitals, these species exhibit comparably low shifts and a large shielding anisotropy (Table 16). The high symmetry in these complexes appears to prohibit larger paramagnetic contributions from the metal d orbitals to the ligand shielding tensors (particularly to σ_{33}). The present study thus suggests that shielding tensors for terminal carbonyl ligands may exhibit a very low anisotropy, and isotropic shifts are large, when the ligand substitution pattern leads to low symmetry in metal coordination and in d-orbital occupation. Regular octahedral structures dominate for d^6 complexes (electronically, this situation holds for three-legged piano-stool complexes as well, if the polyhapto-bound π ligand is considered to occupy three coordination sites[47]). Lower symmetry is preferred by d^4 and d^2 complexes owing to their preferences for effective seven- and eight-coordination, respectively. These d-electron counts therefore often lead to lower symmetry for structures and d orbitals, that is, to conditions that favor large paramagnetic d-orbital contributions to the carbonyl shielding tensors and thus large chemical shifts. Even in six-coordinate 16-electron complexes, d^4 metal centers may feature distorted coordination (e.g., in $[Mo(CO)_2\{S_2CN\text{-}iPr_2\}_2]$[48a] or in $[Mo(OtBu)_2(CO)_2(py)_2]$[48b]). No carbonyl chemical shifts have been determined yet for these species, but one might expect unusual effects arising from polarized metal d orbitals. Rather spectacular deshielded carbonyl ^{13}C shifts of $\delta = 453.6$ and 456.7 have recently been reported by Spencer and Girolami for an intermediate in solution which they characterized as a 16-electron d^2 species $[TiCl_2(CO)_2(dmpe)(\eta^1\text{-dmpe})]$.[49] Whether this is a consequence of an extremely polarized d shell and low-lying virtual orbitals, or whether the species is paramagnetic, remains to be seen.

As the 3d shell is of relatively small radial extent, the d-orbital contributions to the carbonyl shielding tensors are somewhat less pronounced for the Ti and V complexes than for their heavier congeners (see above). This explains at least partially the deviations from the usual "triad behavior" (i.e., increasing shielding of the ligand nuclei down a given triad) for many of these species (see Table 1). The calculations exaggerate the effect to some extent (probably in part due to the neglect of spin–orbit coupling; see Section 2), but the differences between four-legged and three-legged piano-stool complexes clearly support this rationale. We have shown recently that in more "typical" carbonyl complexes like $M(CO)_6$ (M = Cr, Mo, W) the normal "triad effect" is largely due to reduced paramagnetic contributions to $\sigma_\perp$ from C–M σ-bonding orbitals.[18] In these examples, the contributions from occupied metal d orbitals were moderate and almost independent of the metal. This is not quite true for the three-legged d^6 complexes $[MCp(CO)_3]$ (the calculated d-orbital contributions for M = Mn are ca. 10 ppm larger than for M = Tc, Re), and certainly not for the four-legged d^4 complexes (Table 8). We thus should find deviations from the usual "triad behavior" when there are large, metal-dependent contributions from d orbitals. This may be expected to coincide with reduced shielding anisotropy, and to apply also to bridging CO ligands.

Of course, we might expect that the above conditions not only apply to carbonyl ligand shifts, but also to similar ligands, such as isonitriles, thiocarbonyl, etc. Indeed, the bent-sandwich isonitrile complexes $[MCp_2(CO)(CN\text{-}C_6H_3Me_2)]$ exhibit very large nitrile ^{13}C shifts ($\delta = 220$ and 237 for M = Ti, Zr, respectively; note the deviation from normal "triad" behavior).[10b]

We should comment on the relation between the NMR shifts and $d(M) \rightarrow \pi^*(C\equiv O)$ backbonding. Obviously, the presence of suitable, energetically high-lying and spatially extended occupied metal d orbitals is important both for the unusually large CO ligand NMR shifts and for effective backbonding. However, the symmetry conditions involved differ somewhat: while backbonding simply requires good overlap (and energetic match) between metal d orbitals and π^*-C≡O orbitals, large paramagnetic contributions to the carbon and oxygen shielding tensors require the prior action of the magnetic vector potential on the occupied orbitals.[29] Within a sum-over-states ansatz this means that only rotationally allowed electronic transitions contribute to the paramagnetic shielding expression. Thus, while the frequencies of the $\tilde{\nu}$(CO) stretching vibrations are a somewhat more direct measure of backbonding (however, note ref. [50]), the mechanism of ^{13}C and ^{17}O shifts is more complicated (which is also due to the fact that shielding is a tensorial property). This explains the lack of correlation between these different quantities when the molecular structures involved are not similar (see, e.g., Table 2 and refs. [42, 51]).

Much smaller ^{13}C and ^{17}O shielding anisotropy and larger isotropic shifts than in typical terminal carbonyl groups are also found for bridging carbonyl ligands in multinuclear clus-

ters.[36,38,41] Preliminary computational results[41] indicate that, depending on the bonding situation, this is due to paramagnetic contributions from either C–M bonding or from nonbonding or cluster-bonding metal d-orbitals. The latter two cases exhibit obvious analogies to the present work.

Acknowledgment: This work has greatly benefitted from progress made during a stay at Université de Montréal, Canada. I am grateful to Dr. V. G. Malkin and O. L. Malkina (Bratislava) and to Prof. D. R. Salahub (Montréal) for stimulating discussions. Prof. J. E. Ellis (Minneapolis) gave helpful comments on the manuscript. I also thank the NSERC (Canada) and the DFG (Germany) for scholarships, and Prof. H. G. von Schnering (Max-Planck-Institut Stuttgart) and Prof. H.-J. Werner (Universität Stuttgart) for their support and for providing computational resources.

Received: August 8, 1995 [F186]

[1] *^{13}C NMR Data for Organometallic Compounds*, B. E. Mann, B. F. Taylor, Academic Press, London, **1981**.
[2] B. E. Mann in *Multinuclear NMR* (Ed.: J. Mason), Plenum Press, New York, **1987**, pp. 293 ff.
[3] L. J. Todd, J. R. Wilkinson, *J. Organomet. Chem.* **1974**, *77*, 1.
[4] In some nonclassical carbonyl complexes, shifts may be as low as $\delta = 140$. See, e.g., refs. [1, 2].
[5] a) B. Kelsey Stein, J. E. Ellis, *J. Am. Chem. Soc.* **1986**, *108*, 1344. b) B. A. Kelsey, J. E. Ellis, *J. Chem. Soc. Chem. Commun.* **1986**, 331. c) S. R. Frerichs, B. Kelsey Stein, J. E. Ellis, *J. Am. Chem. Soc.* **1987**, *109*, 5558. d) S. R. Frerichs, J. E. Ellis, *J. Organomet. Chem.* **1989**, *359*, C41. e) J. E. Ellis, S. R. Frerichs, B. Kelsey Stein, *Organometallics* **1993**, *12*, 1048. f) J. E. Ellis, B. Kelsey Stein, S. R. Frerichs, *J. Am. Chem. Soc.* **1993**, *115*, 4066. g) K. M. Chi, S. R. Frerichs, B. K. Stein, D. W. Blackburn, J. E. Ellis, *J. Am. Chem. Soc.* **1988**, *110*, 163.
[6] D. W. Blackburn, K.-M. Chi, S. R. Frerichs, M. L. Tinkham, J. E. Ellis, *Angew. Chem.* **1988**, *100*, 408; *Angew. Chem. Int. Ed. Engl.* **1988**, *27*, 437.
[7] T. G. Gardner, G. S. Girolami, *Organometallics* **1987**, *6*, 2551.
[8] G. T. Palmer, F. Basolo, L. B. Kool, M. D. Rausch, *J. Am. Chem. Soc.* **1986**, *108*, 4417.
[9] a) G. Erker, U. Dorf, C. Krüger, K. Angermund, *J. Organomet. Chem.* **1986**, *301*, 299. b) L. J. Procopio, P. J. Carroll, D. H. Berry, *Polyhedron* **1995**, *14*, 45.
[10] a) L. B. Kool, M. D. Rausch, H. G. Alt, M. Herberhold, B. Wolf, U. Thewalt, *J. Organomet. Chem.* **1985**, *297*, 159. b) L. B. Kool, M. D. Rausch, M. Herberhold, H. G. Alt, U. Thewalt, B. Honold, *Organometallics* **1986**, *5*, 2465.
[11] J. E. Ellis, *Adv. Organomet. Chem.* **1990**, *31*, 1.
[12] F. G. N. Cloke, M. F. Lappert, G. A. Lawless, A. C. Swain, *J. Chem. Soc. Chem. Commun.* **1987**, 1667.
[13] J. E. Ellis, K.-M. Chi, *J. Am. Chem. Soc.* **1990**, *112*, 6022.
[14] a) M. Dolg, U. Wedig, H. Stoll, H. Preuss, *J. Chem. Phys.* **1987**, *86*, 866. b) D. Andrae, U. Häußermann, M. Dolg, H. Stoll, H. Preuss, *Theor. Chim. Acta* **1990**, 77, 123.
[15] a) V. G. Malkin, O. L. Malkina, M. E. Casida, D. R. Salahub, *J. Am. Chem. Soc.* **1994**, *116*, 5898. b) V. G. Malkin, O. L. Malkina, L. A. Eriksson, D. R. Salahub in *Theoretical and Computational Chemistry*, Vol. 2 (Eds.: P. Politzer, J. M. Seminario), Elsevier, Amsterdam, **1995**.
[16] M. Kaupp, V. G. Malkin, O. L. Malkina, D. R. Salahub, *Chem. Phys. Lett.* **1995**, *235*, 382.
[17] M. Kaupp, V. G. Malkin, O. L. Malkina, D. R. Salahub, *J. Am. Chem. Soc.* **1995**, *117*, 1851.
[18] M. Kaupp, V. G. Malkin, O. L. Malkina, D. R. Salahub, *Chem. Eur. J.* **1996**, *2*, 24–30.
[19] P. Kubáček, R. Hoffmann, Z. Havlas, *Organometallics* **1982**, *1*, 180.
[20] R. Poli, *Organometallics* **1990**, *9*, 1892.
[21] S. T. Krueger, R. Poli, A. L. Rheingold, D. L. Staley, *Inorg. Chem.* **1989**, *28*, 4599. For an ab initio study on $[(\eta^6\text{-}C_6H_6)M(CO)_3]^+$ (M = Mn, Tc, Re), cf. P. C. Conlon, N. J. Fitzpatrick, *Organometallics* **1994**, *2178*, 173.
[22] A. D. Becke, *Phys. Rev.* **1988**, *A38*, 3098; J. P. Perdew, *ibid.* **1986**, *B33*, 8822.
[23] A. Bergner, M. Dolg, W. Küchle, H. Stoll, H. Preuss, *Mol. Phys.* **1993**, *80*, 1431.
[24] N. Godbout, D. R. Salahub, J. Andzelm and E. Wimmer, *Can. J. Chem.* **1992**, *70*, 560.
[25] M. Pelissier, N. Komiha, J. Daudey, *J. Comput. Chem.* **1988**, *9*, 298.
[26] M. Kaupp, H.-J. Flad, A. Köster, H. Stoll, D. R. Salahub, unpublished results.
[27] C. van Wüllen, *Int. J. Quant. Chem.*, in press.
[28] D. R. Salahub, R. Fournier, P. Mlynarski, I. Papai, A. St-Amant, J. Ushio in *Density Functional Methods in Chemistry* (Eds.: J. K. Labanowski, J. W. Andzelm), Springer, New York, **1991**, p. 77. A. St-Amant, D. R. Salahub, *Chem. Phys. Lett.* **1990**, *169*, 387. A. St-Amant, Thesis, Université de Montréal, **1992**.
[29] W. Kutzelnigg, U. Fleischer, M. Schindler in *NMR-Basic Principles and Progress*, Vol. 23, Springer, Heidelberg, **1990**, pp. 165ff.
[30] J. P. Perdew, Y. Wang, *Phys. Rev.* **1992**, *B45*, 13244; J. P. Perdew in *Electronic Structure of Solids* (Eds. P. Ziesche, H. Eischrig), Akademie Verlag, Berlin, **1991**; J. P. Perdew, J. A. Chevary, S. H. Vosko, K. A. Jackson, M. R. Pederson, D. J. Singh, C. Fiolhais, *Phys. Rev.* **1992**, *B46*, 6671.
[31] A. E. Reed, L. A. Curtiss, F. Weinhold, *Chem. Rev.* **1988**, *88*, 899.
[32] Gaussian 92/DFT, Revision G, M. J. Frisch, G. W. Trucks, M. Head-Gordon, P. M. W. Gill, M. W. Wong, J. B. Foresman, B. G. Johnson, H. B. Schlegel, M. A. Robb, E. S. Replogle, R. Gomperts, J. L. Andres, K. Raghavachari, J. S. Binkley, C. Gonzalez, R. L. Martin, D. I. Fox, D. J. DeFrees, J. Baker, J. P. Stewart, J. A. Pople, Gaussian, Pittsburgh PA, **1992**.
[33] a) M. Hoch, D. Rehder, *Chem. Ber.* **1988**, *121*, 1541. b) W. A. Herrmann, W. Kalcher, H. Biersack, I. Bernal, M. Creswick, *ibid.* **1981**, *114*, 3558. c) M. J. Almond, E. M. Page, D. A. Rice, K. Hagen, H. V. Volden, *J. Mol. Struct.* **1994**, *319*, 223. d) P. J. Fitzpatrick, Y. le Page, I. S. Butler, *Acta Cryst. B* **1981**, *B37*, 1052.
[34] a) M. Kaupp, unpublished results; see also ref. [17]. b) See, e.g., P. Pyykkö, *Chem. Rev.* **1988**, *88*, 563.
[35] M. Y. Darensbourg, *Prog. Inorg. Chem.* **1986**, *33*, 221.
[36] a) J. P. Hickey, J. R. Wilkinson, L. J. Todd, *J. Organomet. Chem.* **1979**, *179*, 159. b) J. P. Hickey, I. M. Baibich, I. S. Butler, *Spectrosc. Lett.* **1978**, *11*, 671. c) D. Cozak, I. S. Butler, J. P. Hickey, L. J. Todd, J. Magn. Res. **1979**, 33, 149. d) Y. Kawada, T. Sugawara, H. Iwamura, *J. Chem. Soc. Chem. Commun.* **1979**, 291. e) S. Aime, D. Osella, L. Milone, G. E. Hawkes, E. W. Randall, *J. Am. Chem. Soc.* **1981**, *103*, 5920.
[37] J. W. Akitt in *Multinuclear NMR* (Ed.: J. Mason), Plenum Press, New York, **1987**, pp. 171 ff.
[38] See, e.g., J. W. Gleeson, R. W. Vaughan, *J. Chem. Phys.* **1983**, *78*, 5384.
[39] E. Oldfield, M. A. Keniry, S. Shinoda, S. Schramm, T. L. Brown, H. S. Gutowsky, *J. Chem. Soc. Chem. Commun.* **1985**, 791.
[40] A. J. Beeler, A. M. Orendt, D. M. Grant, P. W. Cutts, J. Michl, K. W. Zilm, J. W. Downing, J. C. Facelli, M. S. Schindler, W. Kutzelnigg, *J. Am. Chem. Soc.* **1984**, *106*, 7672.
[41] M. Kaupp, unpublished results.
[42] B. E. Mann, *J. Chem. Soc. Dalton Trans.* **1973**, 2012.
[43] R. D. Rogers, J. L. Atwood, M. D. Rausch, D. W. Macomber, *J. Crystallogr. Spectrosc. Res.* **1990**, *20*, 555. H. Plenio, *Chem. Ber.* **1991**, *124*, 2185. H. G. Alt, J. S. Han, R. D. Rogers, *J. Organomet. Chem.* **1993**, *445*, 115. R. Lai, L. Bousquet, A. Heumann, *ibid.* **1992**, *444*, 115.
[44] S. Braun, P. Dahler, P. Eilbracht, *J. Organomet. Chem.* **1978**, *146*, 135.
[45] J. L. Atwood, R. D. Rogers, W. E. Hunter, C. Floriani, G. Fachinetti, A. Ciesi-Villa, *Inorg. Chem.* **1980**, *19*, 3812.
[46] J. W. Lauher, R. Hoffmann, *J. Am. Chem. Soc.* **1976**, *98*, 1729. For more recent photoelectron spectroscopy and DV-X_α results, see: M. Casarin, E. Ciliberto, A. Gulino, I. Fragala, *Organometallics* **1989**, *8*, 900.
[47] In terms of a canonical MO description this means that three occupied fragment MOs of suitable symmetry for an interaction with the metal d orbitals are available; see, e.g., *Orbital Interactions in Chemistry* (T. A. Albright, J. K. Burdett, M.-H. Whangbo), Wiley-Interscience, New York, **1985**, pp. 381 ff. We have recently found that electron localization functions also give a localized visualization of this bonding situation (M. Kaupp, unpublished results).
[48] a) J. L. Templeton, B. C. Ward, *J. Am. Chem. Soc.* **1980**, *102*, 6568. b) M. H. Chisholm, J. C. Huffman, R. L. Kelly, *J. Am. Chem. Soc.* **1979**, *101*, 7615.
[49] M. D. Spencer, G. S. Girolami, *J. Organomet. Chem.* **1994**, *483*, 99.
[50] The C≡O force constants may also be influenced by the σ-C–M bond strength, cf., e.g., M. B. Hall, R. F. Fenske, *Inorg. Chem.* **1972**, *11*, 1619, and references therein.
[51] M. J. Webb, W. A. G. Graham, *J. Organomet. Chem.* **1975**, *93*, 113.

0947-6539/96/0203-0358 $ 15.00+.25/0